An Oxidized Tryptophan Facilitates Copper Binding in *Methylococcus capsulatus*-secreted Protein MopE*[S]

Ronny Helland[‡], **Anne Fjellbirkeland**[§], **Odd Andre Karlsen**[§], **Thomas Ve**[§], **Johan R. Lillehaug**[§], **and Harald B. Jensen**[§1]

From the [‡]*Norwegian Structural Biology Centre, Faculty of Science, University of Tromso, N-9073 Tromso, Norway and the* [§]*Department of Molecular Biology, University of Bergen, N-5020 Bergen, Norway*

Proteins can coordinate metal ions with endogenous nitrogen and oxygen ligands through backbone amino and carbonyl groups, but the amino acid side chains coordinating metals do not include tryptophan. Here we show for the first time the involvement of the tryptophan metabolite kynurenine in a protein metal-binding site. The crystal structure to 1.35 Å of MopE* from the methane-oxidizing *Methylococcus capsulatus* (Bath) provided detailed information about its structure and mononuclear copper-binding site. MopE* contains a novel protein fold of which only one-third of the structure displays similarities to other known folds. The geometry around the copper ion is distorted tetrahedral with one oxygen ligand from a water molecule, two histidine imidazoles (His-132 and His-203), and at the fourth distorted tetrahedral position, the N1 atom of the kynurenine, an oxidation product of Trp-130. Trp-130 was not oxidized to kynurenine in MopE* heterologously expressed in *Escherichia coli*, nor did this protein bind copper. Our findings indicate that the modification of tryptophan to kynurenine and its involvement in copper binding is an innate property of *M. capsulatus* MopE*.

Copper is an essential nutrient for all living organisms, and molecular systems have been developed by all cells to maintain adequate supplies of copper. Copper-containing proteins play a key role in cellular respiration and are involved in biological processes such as pigment formation, neurotransmitter synthesis, and antioxidant defense. Recently, they have received increasing attention due to their role in human pathogenesis, in particular in neurodegenerative diseases such as Alzheimer, Parkinson, and prion diseases (1).

In *Methylococcus capsulatus* (Bath) and other methane-oxidizing bacteria, copper is important for both regulation and

catalytic activity of the particulate methane-monooxygenase (2). An equivalent of this enzyme is used by almost all methanotrophs to catalyze the oxidation of methane to methanol, the initial and obligate step for all carbon fixation and energy production in these bacteria. A subset of methanotrophs, including *M. capsulatus*, produces a second soluble monooxygenase. Soluble monooxygenase does not require copper for activity and is produced only when the level of copper in the growth medium is very low (3, 4). The particulate methane-monooxygenase is the most growth effective of the monooxygenases, and hence, copper is required at relatively high levels for methanotrophs to grow optimally (3). Copper is most likely actively accumulated from the growth medium (3), and thus, the copper-homeostatic activity of methanotrophs differs from that of other prokaryotes in which systems handling extracellular copper is mainly involved in detoxification and elimination (5).

Both methanobactin and the MopE protein have been postulated to have a role in copper uptake in *M. capsulatus* (6, 7). Methanobactin is a small, siderophore-like compound that binds a single copper ion with high affinity (7). When copper is present in the growth medium, methanobactin is mainly associated with the membranes, possibly in direct association with the particulate methane-monooxygenase, whereas at copper-limited growth conditions, methanobactin accumulates in the growth medium. The MopE protein was originally identified as one of five outer membrane-associated proteins, designated MopA-E, Mop being short for M. capsulatus outer membrane protein (8). Later it was discovered that an N-terminal-truncated version (MopE*) of the cell surface-associated protein (MopE[c]) was secreted in large amounts to the growth medium under copper-limited growth conditions (6, 9). MopE[c] is composed of 512 amino acids, whereas MopE* represents the 336 C-terminal amino acids of MopE[c]. A MopE* homologue, designated CorA, has been isolated from the membranes of the methanotroph *Methylomicrobium album* BG8 (10). The expression of both MopE and CorA is negatively regulated by copper, indicating an involvement in copper-homeostatic activities. Importantly, a copper binding motif could not be predicted with significance from the primary sequence of the two proteins (9, 10).

In the present study we determined the crystal structure of MopE* to 1.35 Å of resolution and demonstrate that the protein has a novel protein fold and contains a mononuclear copper site. Importantly, we present evidence that one of amino acids

Oxidized Tryptophan Facilitates Copper Binding

TABLE 1

Data collection and refinement statistics

Values for outer shell are indicated in parenthesis.

	Hg-MopE*	MopE*	Rec-MopE*
Data collection			
Beamline	Bessy, BL14	ESRF, BM01	Bessy, BL14
Wavelength	1.0085	0.8722	0.9184
Detector	MAR CCD165	MAR CCD165	MAR CCD225
Space group	$C2$	$I222$	$C2$
Diffraction limit	1.9	1.35	1.65
No. molecules in asymetric unit	1	1	1
Unit cell parameters			
a axis (Å)	65.92	72.99	65.28
b axis (Å)	101.22	88.57	100.67
c axis (Å)	54.78	101.43	54.65
β-Angle (°)	98.24	90.00	97.56
Total no. of reflections	367,401 (53,094)	368,670 (52,775)	151,184 (15,832)
No. of unique reflections	27,480 (3,963)	71,009 (10,134)	41,358 (5,489)
Completeness (%)	98.2 (97.3)	98.5 (97.3)	98.4 (89.9)
$I/\sigma(I)$	8.4 (1.3)	8.6 (1.6)	7.5 (2.3)
Mean $((I)/S.D. (I))$	24.7 (5.5)	19.4 (3.0)	13.6 (3.3)
R_{merge} (%)	6.9 (55.4)	4.5 (47.6)	5.3 (33.4)
Multiplicity	13.4 (13.4)	5.2 (5.2)	3.7 (2.9)
Wilson B (Å^2)	26.77	14.10	20.14
Outer shell	2.00-1.90	1.42-1.35	1.74-1.65
Structure determination			
Phasing power	0.91		
R_{Cullis}	0.85		
Figure of merit	0.25		
Refinement			
R_{work} (%)	22.11	19.27	18.14
R_{free} (%)	24.48	21.13	20.39
Average B factors (Å^2)	31.00	16.70	21.38
Root mean square deviations			
Bond lengths (Å)	0.022	0.007	0.013
Bond angles (°)	2.347	1.141	1.348
Diffraction-component precision indicator	0.1344	0.0555	0.0834
Ramachandran plot			
In most favored regions (%)	85.2	87.3	87.3
In additional allowed regions (%)	13.9	12.2	12.2
In generously allowed regions (%)	0.8	0.4	0.4

in the copper-binding site is kynurenine, a tryptophan derivate not previously described in protein metal-binding sites.

EXPERIMENTAL PROCEDURES

Growth Conditions and Purification of MopE*—MopE* was obtained from spent medium of *M. capsulatus* (Bath) strain NCIMB 11132 grown in continuous cultures in nitrate mineral salts medium containing no added copper, as described previously (6), and purified as described in the supplemental information.

Protease Treatment and Mass Spectrometry Analyses—MopE* was digested with Lys-C endoproteinase (Roche Applied Science) (11, 12). Mass spectrometric analyses (MALDI-TOF[2] MS and MS/MS) were performed at PROBE, University of Bergen. A detailed description is given in the supplemental information.

Metal Determination—The amount of copper bound per MopE* molecule was determined by inductively coupled plasma mass spectrometry (ICP-MS) at the Center for Element and Isotope Analyses, University of Bergen, Norway (see the supplemental information).

The Copper Binding Affinity of MopE—Information on the dissociation constant of copper binding to MopE* was obtained using the Cu(I) chelator bathocuproine. Bathocuproine disul-

fonic acid (Sigma) and ascorbate were added to MopE* ($\sim$10 μM) in 20 mM Tris-HCl (pH 7.5) and 1 mM CaCl$_2$ to final concentrations of 0.5 and 1 mM, respectively. Ascorbate was included in the assay to ensure that the copper ions were maintained in the Cu(I) state. Samples were incubated either at room temperature or at 45 °C for 1 h with gentle shaking every 5 min. The protein was subsequently isolated using a 5-ml Hitrap desalting column (GE Healthcare), and the concentration of copper in the protein fraction was determined by ICP-MS analyses.

Cloning, Expression, and Purification of MopE in Escherichia coli*—MopE* was amplified by PCR and cloned into the pETM41 vector using BamHI and NcoI restriction sites. Large-scale protein expression was performed using *E. coli* BL21 Star™ (DE3) and the pETM41 vector. Purification of MopE* is described in the supplemental information.

Crystallization, Data Collection, Structure Determination, and Refinement—All variants of MopE* were crystallized from ammonium sulfate in the pH range 7.0–7.75. Data were collected at 100–120 K, and the data were processed in XDS (14), MOSFLM (13), and SCALA and TRUNCATE of the CCP4 suite (15). The structure was phased by single anomalous dispersion techniques using SHELXD (16) on a mercury derivative. The phases were improved by SHARP (17) and solvent flattening using SOLOMON (18). ARP/wARP (19) was used for automatic tracing of the protein, and the model was further

---

[2] The abbreviations used are: MALDI-TOF, matrix-assisted laser desorption ionization time-of-flight; MS, mass spectroscopy; ICP, inductively coupled plasma.
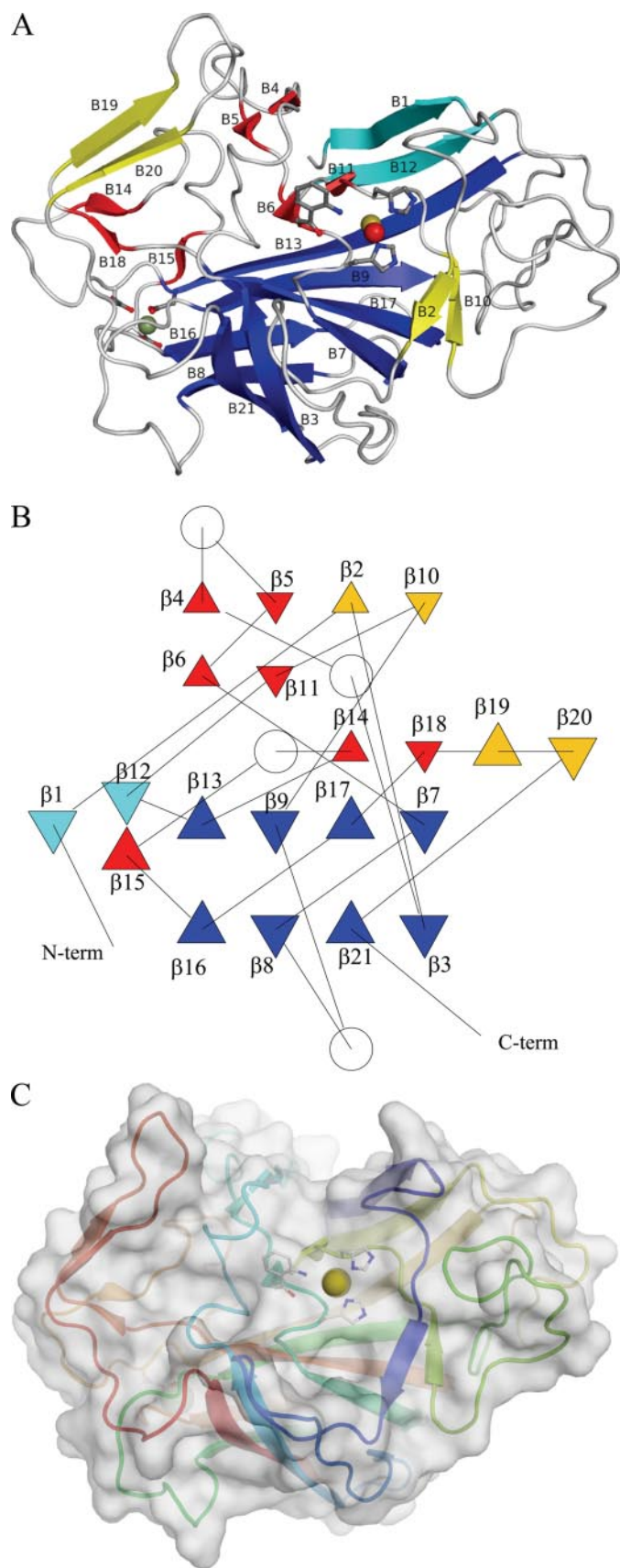
FIGURE 1. *A*, ribbon diagram illustrating the fold of the MopE* structure. The β-strands forming the secondary structure elements of MopE* are labeled B1 through B21, and the coloring follows the topology diagram described below. Copper is represented as a *yellow sphere* located between His-132,

improved by refinement using Refmac5 (21) and manual refitting of the model using O (20). The structures of MopE* and recombinantly expressed in *E. coli* (Rec-MopE*) were solved by molecular replacement using MOLREP (22). A more detailed description of the MopE* structure determination is presented in the supplemental information, and data collection and refinement statistics are summarized in Table 1.

RESULTS

The MopE Structure*—Crystals suitable for x-ray diffraction studies, with different morphology and cell parameters belonging to monoclinic (*C*2) and orthorhombic (*I*222) space groups, were obtained (Table 1 and supplemental Fig. S1). The crystal structure of MopE* was determined using single anomalous dispersion data to 1.9 Å collected on a $HgCl_2$ derivative (Hg-MopE*). The structures of the wild-type protein (MopE*) and MopE* recombinantly expressed in *E. coli* (Rec-MopE*) were determined to 1.35 and 1.65 Å, respectively, by molecular replacement using the mercury derivative as starting model. Data collection and refinement statistics are provided in Table 1. The three structures of MopE* are essentially similar but with a significant difference in the metal-binding site.

The present structure (Fig. 1) includes the 290 C-terminal residues of the protein, and the structures have been refined to crystallographic R-factors of about 18–21% (R_{work}) and R_{free} of 20–24% (Table 1). Main chain atoms of MopE* and Rec-MopE* residues 47–336 superimpose on each other with a root mean square deviation value of 0.57 Å. The differences are caused by the loops formed by residues 75–80 (β2–β3 loop), 105–110 (β3–β4 loop), 115–119 (β4–β5 loop), and 308–312 (β19–β21 loop). Different crystal packing environments in the β2–β3 and β4–β5 loops and poorly defined electron density in the solvent-exposed β19–β20 loops of both proteins are expected to cause the different conformations in three of the four loops. Only the conformation of the β3–β4 loops is expected to be caused by differences in the metal-binding sites of the wild-type and recombinant proteins. The 46 N-terminal amino acids of MopE* were not identified in the electron density maps in any of the structures.

The protein forms a nest-like structure with dimensions of about $40 \times 45 \times 55$ Å^3 (Fig. 1, *A* and *C*). The majority of the MopE* structure folds into a coiled structure where only a third of the residues forms 21 β-strands (Fig. 1*B*). Eight of these build the only extensive secondary structure motif, an antiparallel β-sandwich. The MopE* structure also contains four 3_{10} helical segments. The polypeptide is folded such that regions of the

His-203, kynurenine 130, and a water molecule (*red sphere*) in a tetrahedral arrangement. A single calcium ion (*green sphere*) is coordinated by the side chains of Asp-250, -252, and -274 and the main chain carbonyl oxygen of Thr-276 and Ala-279. *B*, topology diagram (generated at the Topology of Protein Structure (TOPS) server, University of Leeds) illustrating the organization of secondary structure elements of MopE*. *Triangles* represent β-strands, and *circles* represent 3_{10}-helical segments. *Blue triangles* represent the β-sandwich, and *cyan triangles* represent the additional strands forming the central core. *Red triangles* represent strands consisting of only two amino acids. *C*, transparent van der Waals surface, including the ribbon representation, illustrating the crystal structure of MopE*. The *ribbon* is rainbow-colored, where *blue* is at the N terminus of the structure, and *red* is at the C terminus. Copper is represented as a *yellow sphere*.

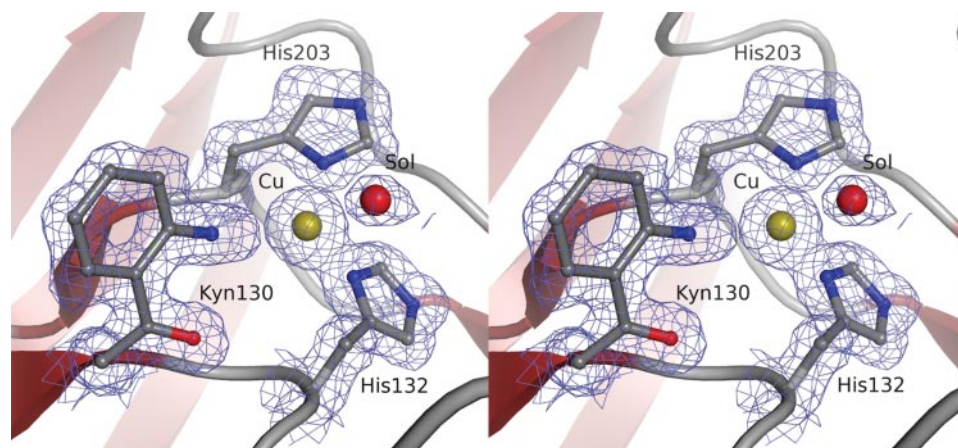# Oxidized Tryptophan Facilitates Copper Binding

FIGURE 2. **Electron density maps of the copper-binding site of MopE*.** The copper and the coordinating water, or hydroxyl, are illustrated as *yellow* and *red spheres*, respectively. The 2fofc electron density is contoured at 1σ.

N-terminal, the middle, and C-terminal parts all are included in the β-sandwich (Fig. 1). One of the strands of the sandwich extends into a second 3-stranded sheet such that the central core of the protein is a 6-stranded sheet. Of the remaining β-strands, seven consist of only two residues each being involved in stabilizing the MopE* structure. The structure is also stabilized by a calcium ion octahedrally coordinated by three aspartic acid residues (Asp-250, Asp-252, Asp-274), two main chain carbonyl oxygens (Thr-276, Ala-279), and a solvent molecule (Fig. 1).

The copper-binding site contains a single partially buried copper ion (Fig. 1*C*) located in a trigonal arrangement by the side groups of His-132, His-203, and intriguingly, Trp-130. Tryptophan has been shown to bind various metals in chemical systems (23, 24); the indole side chain has not been reported to coordinate metal ions in biological systems. The electron density maps revealed a broken bond between the CD1 and NE1 atoms of Trp-130 (Fig. 2). In addition, the planar arrangement around the CG atom and the distances from the atom at the CD1 position to the main chain amine nitrogen atoms of residues 130, 131, and 132 suggested oxidation of the tryptophan to kynurenine. Kynurenines are formed by oxidative cleavage of the tryptophan indole ring with subsequent hydrolysis of the CD1 carbon, resulting in a mass increase of 4 Da compared with the unmodified tryptophan (Fig. 3*B* and supplemental Fig. S2).

The copper ion is also coordinated by an axial water molecule, forming a distorted tetrahedral arrangement of the copper-binding site with the copper ion located almost in the middle of the base of the pyramid and the solvent molecule in the apical position (Fig. 2). Trigonal, tetrahedral, and trigonal bipyramidal are all geometries previously observed for copper-binding proteins (25). The distances between the copper ion and the ND1 atoms of the histidines are in the range 1.99–2.17 Å, indicating covalent/ionic interactions. This is also in the same order as copper-histidine distances found in most other copper-binding proteins (26, 27). The distance between the copper ion and the nitrogen atom of the kynurenine is about 3 Å, somewhat longer than what is usually considered a copper-nitrogen interaction. The amino group of the kynurenine side chain would generally be considered a poor copper ligand. The

amino group is ~6 degrees off a linear phenyl-amino-copper interaction and, as such, does not coincide with a possible amino-metal interaction previously described (25). The copper to solvent distance in MopE* refines to about 2.5 Å, similar to what is found in other copper proteins. The occupancy of the copper ion is refined to about 0.65, which corresponds well with the ICP-MS analyses on purified MopE* revealing a copper-to-protein ratio between 0.5 and 0.6.

Identification of Kynurenine by Mass Spectrometry—To verify the oxidation of tryptophan to kynurenine, purified MopE* was digested with Lys-C, and the resulting peptides were analyzed by MALDI-TOF mass spectrometry. Computer-generated Lys-C peptide maps of MopE* calculated theoretical m/z ions of 2785 and 2789 for tryptophan and kynurenine, respectively. The MS analyses revealed a MALDI molecular ion at m/z 2789, consistent with the theoretically predicted ion for the kynurenine-containing peptide (Fig. 3, *A* and *B*, *upper panels*). Subsequent fragmentation of the m/z 2789 ion produced an MS/MS spectrum corresponding to the amino acid sequence Trp-112—Lys-135 of MopE* (Fig. 3*C*, *left panel*). From both the y-ion and b-ion series it was possible to identify a mass increase of 4 Da at residue 130. No distinct peak was observed at m/z 2785 (Fig. 3, *A* and *B*, *upper panels*).

Analyses of Recombinant MopE—Crystallization and MS studies were also carried out on MopE* heterologously expressed and purified from *E. coli* (Rec-MopE*). The MS spectrum and MS/MS fragmentation pattern on peptides derived from Rec-MopE* revealed solely the unmodified m/z 2785 peptide, demonstrating that the post-translational formation of kynurenine in MopE* had not occurred when expressed in *E. coli* (Fig. 3, *A* and *B*, *lower panels*, and *C*, *right panel*). This was confirmed by crystal structure analysis of Rec-MopE*. The electron density clearly displayed an intact CD1–NE1 bond (Fig. 4*A*). In addition, the side chain was rotated about 60 degrees in χ1 and 180 degrees in χ2 relative to kynurenine in wild-type MopE* (Fig. 4*B*). To accommodate the tryptophan side chain in this position, the β3–β4 loop (residues 105–110) is displaced about 1.5 Å. Thus, the metal-binding site is sufficiently disrupted to prevent binding of copper in Rec-MopE*, as demonstrated by the lack of electron density at the wild-type copper position. The latter was confirmed by ICP-MS; Rec-MopE* did not bind detectable levels of copper. These findings substantiate that the conversion of tryptophan to kynurenine is an endogenous modification that specifically takes place in *M. capsulatus* and that the oxidation of Trp-130 to kynurenine is a prerequisite for copper binding in wild-type MopE*.

The Copper Binding Affinity of MopE—Bathocuproine disulfonic acid was used to obtain information on the copper binding affinity of MopE*. Bathocuproine disulfonic acid forms a stable 2:1 complex with Cu(I) with an association constant of
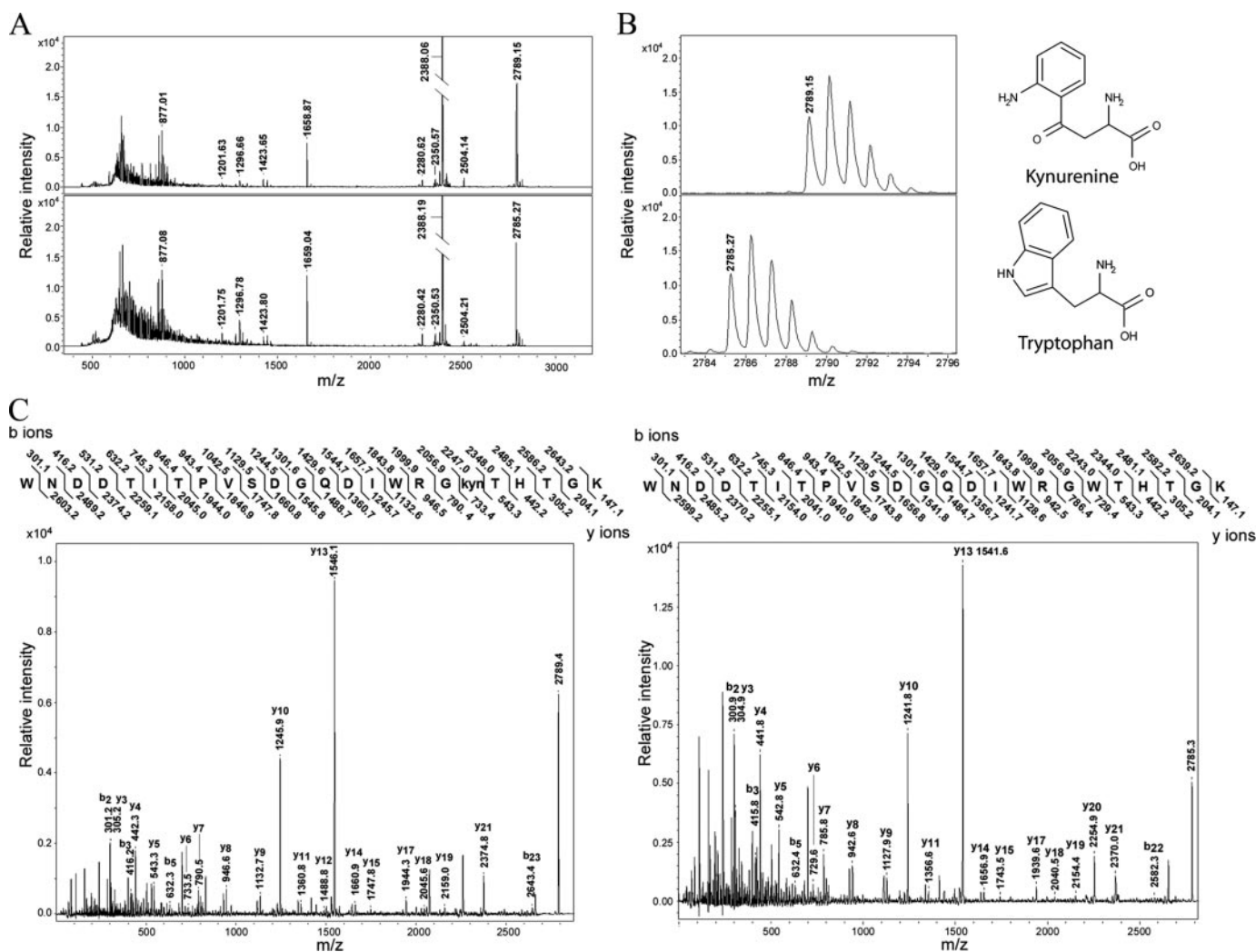
FIGURE 3. **MALDI-MS spectra.** *A*, MALDI-MS spectra of Lys-C produced peptides from MopE* (*upper*) and Rec-MopE* (*lower*) isolated from *M. capsulatus* and *E. coli*, respectively. Monoisotopic peaks are labeled with their respective *m/z* ratio. *B*, MALDI spectra (mass range 2783–2796 Da) of *A*) showing the *m/z* 2789 (*upper*) and *m/z* 2785 (*lower*) ions. *Right-hand side*, chemical structures of kynurenine and tryptophan. *C*, tandem mass spectra of the *m/z* 2789 ion (*left panel*) and the *m/z* 2785 ion (*right panel*), indicating the observed fragmentation pattern and the sequence ion assignments. Predicted ions are shown at top of the figures, where a 4-Da increase in mass at Trp-130 is considered for the *m/z* 2789 ion. The oxidized tryptophan is displayed as *kyn* in the amino acid sequence of the 2789-Da peptide.

$\sim 10^{20}$ (28). No significant decrease in the amount of copper bound to MopE* could be observed after treatment with the copper chelator either at room temperature or at 45 °C, thus indicating a high affinity binding ($K_d < 10^{-20}$ M).

DISCUSSION

We present here x-ray diffraction and mass spectrometry data on the *M. capsulatus*-secreted protein, MopE*. The protein presents a unique kynurenine-containing copper-binding site and a novel protein fold, of which only about a third of the MopE* structure displays similarity to known proteins. The only extensive secondary structure element previously observed is an 8-stranded antiparallel β-sandwich formed by about 25% of the residues. This motif is often found in virus capsid proteins and sugar binding and hydrolyzing proteins as well as in oxidoreductases, cupredoxins (proteins with Type I copper center), and proteins involved in electron transport (DALI data base (29), ProFunc (30), and CATH protein classification data base (31)). The remaining residues form an exten-

sive coil-like structure interspersed with 13 short β-strands. Particularly interesting is the copper-binding site located in a depression on the molecular surface about 8–10 Å from the β-sandwich and relatively distant from any secondary structure element. The partially buried copper ion is located between two histidines and an oxidized tryptophan (kynurenine) in a planar trigonal arrangement and displays, therefore, similarities to Type I (blue copper proteins) and Cu_B copper centers (25, 32). Type I copper centers are characterized by two histidines and a cysteine in a planar trigonal arrangement and a variable axial ligand. Cu_B copper centers coordinate copper by three histidines in a trigonal pyramidal geometry, and the axial ligand forms a bridge to the iron ion of the cytochrome heme. Two and three histidine ligands are frequently observed in copper-binding proteins, but to our knowledge this is the first observation of a tryptophan or a tryptophan metabolite involved in metal binding.

When previously detected in proteins, kynurenine was considered the result of oxidative damage, and in most studies on proteins containing modified tryptophan residues, the kynu-
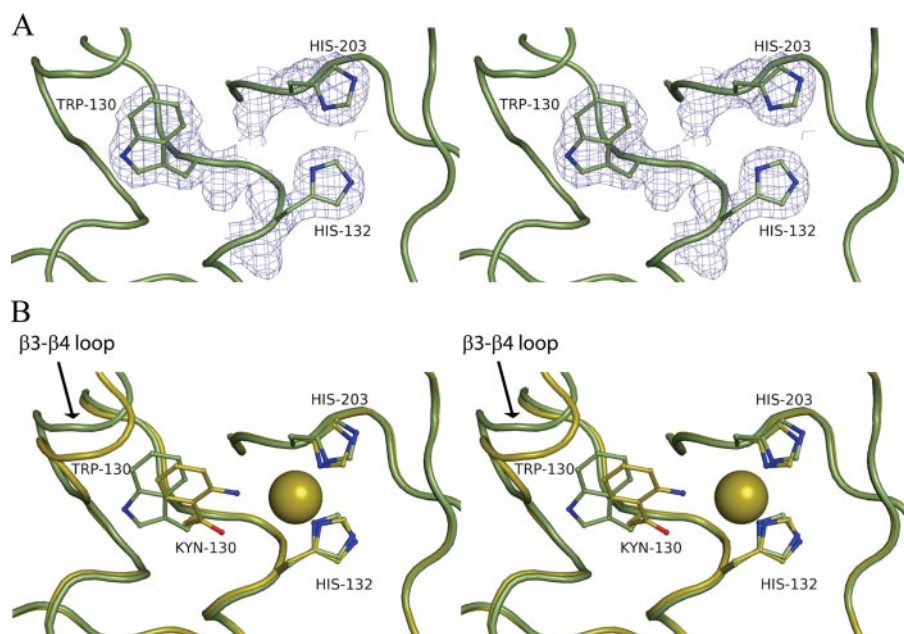
FIGURE 4. *A*, electron density maps covering the residues forming the copper-binding site of Rec-MopE*. The 2fofc electron density is contoured at 1σ and shows that Trp-130 is in its unoxidized state. *B*, MopE* (*yellow*) superimposed on Rec-MopE* (*green*). Trp-130 in Rec-MopE* is rotated relative to Kyn130 in MopE. The copper found in MopE* is illustrated as a *yellow sphere*.

renine modification was formed by exposing the proteins to oxidative stress *in vitro* (33–35). There is accumulating evidence that oxidation of specific tryptophan residues takes place *in vivo* (36–40), but evidence for biological functions of kynurenines in proteins has to our knowledge not been presented. Structural evidence by NMR for naturally occurring kynurenine has been provided only for the antibiotic peptide daptomycin (37, 38) from *Streptomyces roseosporus*. In other studies on kynurenine-containing proteins, kynurenine was detected by MS analyses, and for all proteins examined the MS spectra revealed two distinct peaks with m/z corresponding to oligopeptides containing both unmodified and modified tryptophan residues (35, 36, 39, 40). We did not detect the tryptophan signature peak at m/z 2785 in the mass spectrum of MopE* (Fig. 3, *A* and *B*) in our present study. This indicates that oxidation of the specific tryptophan to kynurenine in MopE* is highly efficient in *M. capsulatus.* The mass increase of 4 Da observed for the modified tryptophan is compatible with an opening of the indole ring resulting in an amino group attached to the phenyl ring and a methyl group at the aliphatic chain (supplemental Fig. S2C), but this would not be consistent with the planar arrangement observed around the atom corresponding to the CG position of a Trp-130. A methylene group would fit the planar arrangement (supplemental Fig. S2D), but this molecule would present a mass increase of 2 Da relative to tryptophan. The relatively short distances from the atom at the possible methyl group corresponding to the Trp-130 CD1 position and the main chain nitrogen atoms of residues 131–133 (2.9–3.2 Å) correspond more to hydrogen bond distances than a polar-nonpolar N-C interaction. Thus, our x-ray diffraction data are consistent with the presence of kynurenine also in the MopE* crystals.

Metal binding distances are generally considered a function of the size, ionization, and electron donating properties of the ligand. The distance between the copper ion and the nitrogen atom of the kynurenine is about 3 Å, considerably longer than what is usually considered a copper-nitrogen interaction, which is 2–2.3 Å (see *i.e.* (26, 41)), and longer than some of the longest Cu–N bonds reported previously (in non-biological systems; 2.8 Å (42)). The kynurenine is, therefore, probably not a first-sphere ligand, but the ring amino group is close enough to be a second sphere copper ligand.

The copper content of purified MopE* and crystallized MopE* were similar (0.5–0.6 and 0.65 copper per molecule MopE*, respectively), which was less than what would be expected given the high copper affinity determined for MopE*. Purified MopE* was unable to bind additional copper, added either as Cu^+ or Cu^{2+} (data not shown). The actual copper content of purified MopE* was found by ICP-MS analysis to depend largely on the copper content of the growth medium but did not exceed about 80% of the sites.

In contrast, when co-crystallizing MopE* (Cu-MopE*) with 10 mM $CuSO_4$, the occupancy of copper increased from ~65% to 100%. Under copper-containing conditions crystals belonging to a new monoclinic space group (C2; 104.11 × 101.58 × 38.64 Å³, β = 101.40°) have been obtained. These crystals diffracted to 1.6 Å (data not shown). The addition of copper to the crystallization conditions had only minor effects on the binding distances, with differences to the neighboring amino acids less than 0.1 Å. The copper-binding site is open to the solvent in both crystal forms and should in principle not be significantly influenced by close crystal packing interactions. The differences are in the same order as the coordinate error (0.06 Å–0.08 Å), and hence, no trend related to copper occupancy could be drawn.

A possible explanation for the difference in metal binding capacity between purified (65%) and crystallized MopE* (65–100%) could be related to structural differences and may to some degree reflect the amount of copper bound during expression and retained through purification. In the crystal, the 46 N-terminal amino acids are invisible in the electron density maps in all crystal forms, suggesting that this domain is unstructured or cleaved off during the crystallization process. We hypothesize that in solution the N-terminal domain of MopE* may serve as a lid regulating/inhibiting further metal binding. Removal of this domain would expose the binding site to the solvent, allowing copper binding in all sites.

The kynurenine amino group is ~6 degrees off a linear phenyl-amino-copper interaction and as such does not fit the amino-metal interaction requirements described by Holm *et al.* (25). The kynurenine residue is, therefore, apparently not a ligand in the classical sense, and at present we can only specu-

late about the function of kynurenine in the copper-binding site of MopE*. Because the Trp-130 of MopE* expressed in *E. coli* is not oxidized and this protein does not bind copper either in solution or in crystals grown in the presence of copper, it is likely that the conformational changes that take place as a consequence of Trp-130 oxidation to kynurenine is a requisite for copper binding. The solvent-exposed indole side chain of Trp-130 in Rec-MopE* is stabilized only by a hydrogen bond to Asp-105 and by weak hydrophobic interactions to neighboring residues. After oxidation, rotation of the kynurenine side chain allows stabilization of the carbonyl oxygen through hydrogen bonds to the main chain amine nitrogen atoms of residues 131–133. Kynurenine in this conformation reduces the size and flexibility of the otherwise relatively open copper-binding site, possibly providing a structural pocket for entrapment of the copper ion and, thus, ensuring efficient covalent/ionic binding to the histidine ligands.

The chemical properties of Trp are considered incompatible with direct metal-coordination in biological systems (24). Consistent with this, the *E. coli* expressed Rec-MopE* containing only unmodified Trp-130 did not bind detectable levels of copper. The lack of Trp modification in Rec-MopE* is intriguing because it suggests that this modification is enzymatically mediated and consequently most likely requires another protein(s) to catalyze the reaction. In this respect, it is interesting that the *mopE* gene (MCA2589) is located in an operon with the MCA2590 gene encoding a protein displaying sequence similarity to the tryptophan-modifying MauG proteins (6, 43). The MauG proteins are c-type cytochromes that are required for biosynthesis of tryptophan tryptophylquinone, the prosthetic group of methylamine dehydrogenase (44, 45). The *M. capsulatus* MauG homologue is, like MopE*, located on the surface of the bacterium and is a member of a novel group of the bacterial di-heme cytochrome *c* peroxidase family with unknown function (43). The MCA2590-encoded cytochrome may be active in the conversion of Trp-130 to kynurenine, but this possibility remains to be investigated. Interestingly, a protein with 50% sequence similarity to the *M. capsulatus* MCA2590-encoded cytochrome is predicted from an unannotated ORF located immediately downstream of CorA, the MopE* homologue produced by the methanotroph *Methylomicrobium* album BG8 ((10) see below).

The structure of MopE* displays little resemblance to known copper proteins, and the function can, therefore, not be predicted from the structure. To date, the copper-repressible CorA protein is the only known MopE homologue. CorA is composed of 204 amino acids, all of which can be aligned to the C-terminal region (amino acids 56–336) of MopE* (9) and with conserved residues around the metal-binding sites (supplemental Fig. S3). Also, the three aspartic acid residues that contribute side chain coordinates for the calcium ion in MopE* (Fig. 1, supplemental Fig. S3) are conserved in CorA. Thus, circumstantial evidence indicates that MopE and CorA have a related function in copper homeostatic activities. Because MopE is copper-repressed and has a very high affinity for copper, it is tempting to speculate that MopE plays a role in copper uptake and transport at low copper culture conditions. Very little information about

copper uptake in methanotrophs is available. The only molecule in addition to MopE that has been linked to copper transport in these bacteria is methanobactin (7). Like MopE*, methanobactin is accumulated in the medium at low copper growth conditions and binds a single copper with high affinity, similarly to MopE*. A low K_d would be expected for a copper-binding protein operating in a low copper environment. If MopE is involved in copper transport, a copper receptor is likely to exist at the cellular surface, but candidate molecules mediating intracellular transport remain to be identified, and characterization of MopE participation in copper homeostasis must await further studies.

The finding of kynurenine as oxidized tryptophan residues in biological systems has so far been described from studies related to oxidative stress or exposure to reactive oxygen species (33–40). In the case of *E. coli*-expressed MopE*, Trp-130 was not oxidized to kynurenine when exposed to strong oxidizing conditions. This could indicate that the oxidation of Trp-130 in *M. capsulatus* is enzymatically catalyzed. If so, it is tempting to speculate that MopE* is involved in a redox process important for the uptake of copper ions, which most likely takes place at the surface of the bacterium. Involvement in a transport process would explain the reason for choosing a weak ligand, such as kynurenine, because easier transfer of the copper ion to its receptor molecule would be anticipated. The receptor molecule would still have to induce chemical and/or conformational changes to MopE* to release the copper ion. Experiments are initiated to elucidate these questions and unravel whether the role of kynurenine in copper binding is a unique trait of MopE restricted to proteins of methane-oxidizing bacteria or whether it is a more frequent structural feature in biological metal coordination.

The identification of the kynurenine reported here is an important observation of a structural difference between a wild-type protein and its heterologously expressed counterpart. It, thus, provides a warning example that a heterologously expressed protein does not always exert the same properties as that from the wild-type organism. In the case of MopE, the modification takes place only when endogenously expressed in *M. capsulatus* and, thus, appears to be linked to its biological function. In this case the general use of recombinant proteins for structure studies may have made the detection of the kynurenine elusive.

REFERENCES

1. Gaggelli, E., Kozlowski, H., Valensin, D., and Valensin, G. (2006) *Chem. Rev.* **106,** 1995–2044
2. Hakemian, A. S., and Rosenzweig, A. C. (2007) *Annu. Rev. Biochem.* **76,** 223–241
3. Choi, D. W., Kunz, R. C., Boyd, E. S., Semrau, J. D., Antholine, W. E., Han, J. I., Zahn, J. A., Boyd, J. M., de la Mora, A. M., and DiSpirito, A. A. (2003) *J. Bacteriol.* **185,** 5755–5764

4. Murrell, J. C., McDonald, I. R., and Gilbert, B. (2000) *Trends Microbiol.* **8,** 221–225

5. Rensing, C., and Grass, G. (2003) *FEMS Microbiol. Rev.* **27,** 197–213

6. Karlsen, O. A., Berven, F. S., Stafford, G. P., Larsen, O., Murrell, J. C., Jensen, H. B., and Fjellbirkeland, A. (2003) *Appl. Environ. Microbiol.* **69,** 2386–2388

7. Kim, H. J., Graham, D. W., DiSpirito, A. A., Alterman, M. A., Galeva, N., Larive, C. K., Asunskis, D., and Sherwood, P. M. (2004) *Science* **305,** 1612–1615

8. Fjellbirkeland, A., Kleivdal, H., Joergensen, C., Thestrup, H., and Jensen, H. B. (1997) *Arch. Microbiol.* **168,** 128–135

9. Fjellbirkeland, A., Kruger, P. G., Bemanian, V., Hogh, B. T., Murrell, J. C., and Jensen, H. B. (2001) *Arch. Microbiol.* **176,** 197–203

10. Berson, O., and Lidstrom, M. E. (1997) *FEMS Microbiol. Lett.* **148,** 169–174

11. Shevchenko, A., Wilm, M., Vorm, O., and Mann, M. (1996) *Anal. Chem.* **68,** 850–858

12. Gobom, J., Nordhoff, E., Mirgorodskaya, E., Ekman, R., and Roepstorff, P. (1999) *J. Mass Spectrom.* **34,** 105–116

13. Powell, H. R. (1999) *Acta Crystallogr. D Biol. Crystallogr.* **55,** 1690–1695

14. Kabsch, W. (1993) *J. Appl. Crystallogr.* **26,** 795–800

15. Collaborative Computational Project (1994) *Acta Crystallogr. D Biol. Crystallogr.* **50,** 760–763

16. Schneider, T. R., and Sheldrick, G. M. (2002) *Acta Crystallogr. D Biol. Crystallogr.* **58,** 1772–1779

17. De la Fortelle, E., and Bricogne, G. (1997) *Methods Enzymol.* **276,** 472–494

18. Abrahams, J. P., and Leslie, A. G. (1996) *Acta Crystallogr. D Biol. Crystallogr.* **52,** 30–42

19. Perrakis, A., Morris, R., and Lamzin, V. S. (1999) *Nat. Struct. Biol.* **6,** 458–463

20. Jones, T. A., Zou, J. Y., Cowan, S. W., and Kjeldgaard, M. (1991) *Acta Crystallogr. A* **47,** 110–119

21. Murshudov, G. N., Vagin, A. A., and Dodson, E. J. (1997) *Acta Crystallogr. D Biol. Crystallogr.* **53,** 240–255

22. Vagin, A., and Teplyakov, A. (1997) *J. Appl. Crystallogr.* **30,** 1022–1025

23. Kaminskaia, N. V., and Kostic, N. M. (2001) *Inorg. Chem.* **40,** 2368–2377

24. Takani, M., Takeda, T., Yajima, T., and Yamauchi, O. (2006) *Inorg. Chem.* **45,** 5938–5946

25. Holm, R. H., Kennepohl, P., and Solomon, E. I. (1996) *Chem. Rev.* **96,** 2239–2314

26. Harding, M. M. (2006) *Acta Crystallogr. D Biol. Crystallogr.* **62,** 678–682

27. Rulisek, L., and Vondrasek, J. (1998) *J. Inorg. Biochem.* **71,** 115–127

28. Xiao, Z., Loughlin, F., George, G. N., Howlett, G. J., and Wedd, A. G. (2004) *J. Am. Chem. Soc.* **126,** 3081–3090

29. Holm, L., and Sander, C. (1996) *Science* **273,** 595–603

30. Laskowski, R. A., Watson, J. D., and Thornton, J. M. (2005) *Nucleic Acids Res.* **33,** W89–W93

31. Orengo, C. A., Michie, A. D., Jones, S., Jones, D. T., Swindells, M. B., and Thornton, J. M. (1997) *Structure* **5,** 1093–1108

32. Solomon, E. I., Sundaram, U. M., and Machonkin, T. E. (1996) *Chem. Rev.* **96,** 2563–2606

33. Yang, C., Gu, Z. W., Yang, M., Lin, S. N., Siuzdak, G., and Smith, C. V. (1999) *Biochemistry* **38,** 15903–15908

34. Zhang, H., Joseph, J., Crow, J., and Kalyanaraman, B. (2004) *Free Radic. Biol. Med.* **37,** 2018–2026

35. Manzanares, D., Rodriguez-Capote, K., Liu, S., Haines, T., Ramos, Y., Zhao, L., Doherty-Kirby, A., Lajoie, G., and Possmayer, F. (2007) *Biochemistry* **46,** 5604–5615

36. Anderson, L. B., Maderia, M., Ouellette, A. J., Putnam-Evans, C., Higgins, L., Krick, T., MacCoss, M. J., Lim, H., Yates, J. R., III, and Barry, B. A. (2002) *Proc. Natl. Acad. Sci. U S A.* **99,** 14676–14681

37. Ball, L. J., Goult, C. M., Donarski, J. A., Micklefield, J., and Ramesh, V. (2004) *Org. Biomol. Chem.* **2,** 1872–1878

38. Jung, D., Rozek, A., Okon, M., and Hancock, R. E. (2004) *Chem. Biol.* **11,** 949–957

39. Moller, I. M., and Kristensen, B. K. (2006) *Free Radic. Biol. Med.* **40,** 430–435

40. Taylor, S. W., Fahy, E., Murray, J., Capaldi, R. A., and Ghosh, S. S. (2003) *J. Biol. Chem.* **278,** 19587–19590

41. Harding, M. M. (1999) *Acta Crystallogr. D Biol. Crystallogr.* **55,** 1432–1443

42. Wang, Z. M., Luo, J., Sun, B. W., Yan, C. H., Gao, S., and Liao, C. S. (2000) *Acta Crystallogr. Sect. C Cryst. Struct. Commun.* **56,** 786–788

43. Karlsen, O. A., Kindingstad, L., Angelskar, S. M., Bruseth, L. J., Straume, D., Puntervoll, P., Fjellbirkeland, A., Lillehaug, J. R., and Jensen, H. B. (2005) *FEBS J.* **272,** 6324–6335

44. McIntire, W. S., Wemmer, D. E., Chistoserdov, A., and Lidstrom, M. E. (1991) *Science* **252,** 817–824

45. Pearson, A. R., De La Mora-Rey, T., Graichen, M. E., Wang, Y., Jones, L. H., Marimanikkupam, S., Agger, S. A., Grimsrud, P. A., Davidson, V. L., and Wilmot, C. M. (2004) *Biochemistry* **43,** 5494–5502

SUPPLEMENTAL EXPERIMENTAL PROCEDURES.

Purification of M. capsulatus (Bath) *MopE**. MopE* was obtained from spent medium of *M. capsulatus* (Bath) strain NCIMB 11132 grown in continuous cultures in NMS medium containing no added copper, as described previously (1). Spent medium was obtained by centrifugation of cell cultures at $10,500 \times g$ for 20 minutes. The medium was gently decanted from the cell pellet and filtrated through a 0.45 µM Durapore membrane (Millipore). The supernatant was either kept at –20°C (long time storage) or at 4°C (short time storage). Filtrated supernatant was concentrated approximately 400 times by centrifugation through Amicon® Ultra-PL-100 centrifugation filter devices with a nominal molecular weight limit of 10 kDa (Millipore), and subjected to size exclusion chromatography. 1 – 2 mL of concentrated MopE* was loaded on a Hiload Superdex TM 75 prep grade column (Amersham Biosciences) equilibrated with 20 mM Tris-HCl, pH 7.5, 1 mM CaCl$_2$. Protein was eluted in the same buffer at a flow rate of 1mL/min and 1 mL fractions were collected.

Cloning expression and purification of MopE* in E. coli. mopE* was amplified by PCR (primers: MopE*_F_*Nco*I,   5'-CCATGGGCCTGGACACGCTG-3'; MopE*_*Bam*H1,   5'-GCAGGGATCCATTTACGGCTTGGAGATCGTG-3') and cloned into the pETM41 vector using *Bam*HI and *Nco*I restriction sites, thereby fusing *mopE** to the *mbp* gene separated by a linker region. The *Nco*I cleavage site introduced an additional methionine residue at the N terminal of MopE*. The linker region contains a His-tag and the sequence for the TEV-protease cleavage site. Positive clones were verified by sequencing. Large-scale protein expression was performed using *E. coli* BL21 StarTM (DE3) containing the pETM41 expression vector; The cultures were grown aerobically to mid-exponential phase (A$_{600}$ ≈ 0.6) at 37°C at a shaking speed of 250 rpm, and induced with 1 mM isopropyl thio-β-d-galactoside (IPTG). After overnight incubation at 18°C the cells were harvested and the soluble fraction was isolated following sonication in 50 mM Tris-HCl pH 7.5, 0.1 M NaCl, 10 mM CaCl$_2$, 0.4 mM AEBSF-hydrochloride (Applichem), and 10 mM imidazole. After centrifugation at 15,000g for 20 min, the supernatant was filtered (0.22 µm) before the use of a HisTrapTM chelating column (GE Healthcare). Bound proteins were eluted by a linear gradient of imidazole (10 – 250 mM) in 50 mM Tris-HCl pH 7.5, 0.1 M NaCl, and 10 mM CaCl$_2$. Fractions containing the MBP–(MopE*) fusion protein were pooled and run on a Superdex 75 16 / 60 gel filtration column for further purification and removal of imidazole (gel filtration buffer: 50 mM Tris / HCl pH 7.5, 500 mM NaCl, and 1 mM CaCl$_2$. TEV-protease (Invitrogen, Carlsbad, CA, USA) was added to a concentration of 10 units for 20 µg substrate and incubated at room temperature overnight. His-tagged TEV and MBP were selectively removed by reloading the solution onto the HisTrapTM chelating column where they were tightly bound, whereas MopE* was recovered in the unbound fractions. A final gel filtration of MopE* was performed on a Superdex 75 16 / 60 column to remove traces of imidazole.

Protease treatment and mass spectrometry analyses. MopE* and Rec-MopE* separated by SDS-PAGE were excised from gels and washed twice in 50 mM ammonium bicarbonate and 50% acetonitrile. Prior to protease treatment the washed gel-pieces were dehydrated by vacuum centrifugation and subsequently treated with DTT and iodoacetamide for reduction and alkylation of cysteines as described by Shevchenko et al. 1996 (2). "In gel" digestion of MopE* with the Lys-C endoproteinase was carried out essentially as described by the manufacturer (Roche, Penzberg, Germany). The digested peptides were purified and concentrated as described by Gobom et al. 1999 (3), and MALDI-TOF MS and MS/MS analyses was performed with an Ultraflex mass spectrometer (Bruker Daltronics), and a matrix solution consisting of 8 µg/µL alfa-cyano-4-hydroxycinnamic acid, 60% acetonitrile, 15% methanol, and 0.1% trifluoracetic acid at the PROBE facilities at the University of Bergen.

Metal determination. The amount of copper bound per MopE* molecule was determined by Inductively Coupled Plasma Mass Spectrometry (ICP-MS) at the Centre for Element and Isotope Analyses (CEIA), University of Bergen, Norway.

Prior to the analyses, contaminating metal ions from the gel filtration buffer was removed by dialysing twice (Slide-A-Lyzer, 10,000 MWCO from Pierce) against a 50 times larger volume of 20 mM Tris-HCl, 1 mM $CaCl_2$ pH 7.5. The dialysis was carried out for approximately 24 hours at 4°C. After dialysis the samples were hydrolyzed with nitric acid (6% v/v) overnight on a hotplate (110°C). A single collector double focusing magnetic sector field ICP-MS spectrometer (Finnigan Element 2) was used for the copper analyses.

Crystallization, data collection, structure determination and refinement. Initial screening of crystallization conditions were carried out with Hampton crystallization screens using the Impax crystallization robot from Douglas Instruments. Optimization of conditions was performed using the hanging drop vapor diffusion technique at room temperature. All drops were generated by mixing 2.0 μl of the protein (3 mg/ml dissolved in 20 mM Tris buffer pH 7.5 and 1 mM $CaCl_2$) with 2.0 μl of a precipitant solution and equilibrated against 1.0 ml of the precipitant solution. Crystals suitable for X-ray diffraction studies were obtained from 36 – 45 % ammonium sulfate and 0.1 M Hepes buffer in the pH range 7.25 – 7.75. Recombinant Mope* was crystallized from 36 – 45% ammonium sulfate and slightly lower pH, BisTris buffer at pH 7.0, and 1 – 2 % glycerol added to the reservoir. Heavy atom derivatives were obtained by co-crystallizing MopE* with 1 – 10 mM of the heavy atom included in the reservoir solution. Native and heavy atom derivative X-ray data for MopE* were collected at ID23 and ID 29 at European Synchrotron Radiation Facilities (ESRF), Swiss-Norwegian Beamlines (SNBL) at ESRF, Swiss Light Source and BL14.1 at Bessy. Prior to data collection, all crystals were soaked in cryo solutions identical to the reservoir, but with 25% glycerol included. Data (Table 1) were processed in MOSFLM (4), XDS (5) and SCALA and TRUNCATE of the CCP4 program suite(6). The crystal structure was solved using the single anomalous dispersion (SAD) technique using X-ray data to 1.9 Å collected on a $HgCl_2$ derivative (Hg-MopE*) 10 eV above the Hg L-III edge (1.0085 Å). SHELXD (7) was used to identify two heavy atom sites, and these were further refined with SHARP (8). The phases were improved by solvent flattening using SOLOMON (9; SI Fig. S4). Automatic tracing of the polypeptide chain was carried out with ARP/wARP (10). Subsequent improvement of the model was made by manual refitting of side chains using O (11) based on sigmaA-weighted 2mFo-DFc and mFo-DFc electron density maps. Refinement was carried out in Refmac5 (12) of the CCP4 suite (Table 1). The structures of wild-type MopE*and recombinantly expressed MopE* (Rec-MopE*) were solved by molecular replacement in MOLREP (13) using Hg-MopE* as starting model.

SUPPLEMENTAL REFERENCES

1. Karlsen, O. A., Berven, F. S., Stafford, G. P., Larsen, O., Murrell, J. C., Jensen, H. B., and Fjellbirkeland, A. (2003) *Appl Environ Microbiol* **69**(4), 2386-2388
2. Shevchenko, A., Wilm, M., Vorm, O., and Mann, M. (1996) *Anal Chem* **68**(5), 850-858
3. Gobom, J., Nordhoff, E., Mirgorodskaya, E., Ekman, R., and Roepstorff, P. (1999) *J Mass Spectrom* **34**(2), 105-116
4. Powell, H. R. (1999) *Acta Crystallogr D Biol Crystallogr* **55**(Pt 10), 1690-1695
5. Kabsch, W. (1993) *J Appl Crystallogr* **26**, 795-800
6. Collaborative Computational Project, N. (1994) *Acta Crystallogr D Biol Crystallogr* **50**(Pt 5), 760-763
7. Schneider, T. R., and Sheldrick, G. M. (2002) *Acta Crystallogr D Biol Crystallogr* **58**(Pt 10 Pt 2), 1772-1779
8. De la Fortelle, E., and Bricogne, G. (1997) *Methods in enzymology* **276**, 472-494
9. Abrahams, J. P., and Leslie, A. G. (1996) *Acta Crystallogr D Biol Crystallogr* **52**(Pt 1), 30-42
10. Perrakis, A., Morris, R., and Lamzin, V. S. (1999) *Nat Struct Biol* **6**(5), 458-463
11. Jones, T. A., Zou, J. Y., Cowan, S. W., and Kjeldgaard. (1991) *Acta Crystallogr A* **47** (**Pt 2)**, 110-119

12.   Murshudov, G. N., Vagin, A. A., and Dodson, E. J. (1997) *Acta Crystallogr D Biol Crystallogr* **53**(Pt 3), 240-255

13.   Vagin, A., and Teplyakov, A. (1997) *J Appl Crystallogr* **30**, 1022-1025

LEGENDS TO SUPPLEMENTAL FIGURES

Supplemental **fig. S1**. Crystals of MopE*, from left to right, co-crystallized with 10 mM HgCl$_2$, wild-type MopE* and recombinant MopE*.

Supplemental fig. S2. Chemical representation of tryptophan, kynurenine and two other tryptophan metabolites. The increases in molecular weight relative to tryptophan and the IUPAC names of the compounds are given.
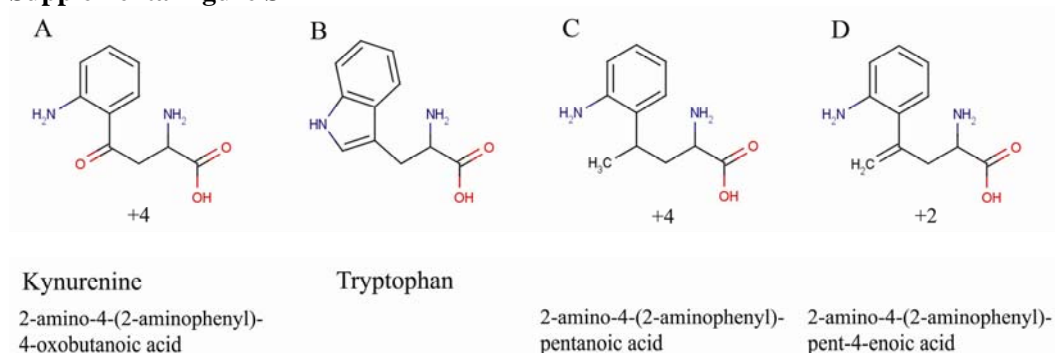
Supplemental fig. S3. Sequence alignment of MopE* with the *M. album* CorA protein. Secondary structure elements, obtained from the MopE* crystal structure, are given above the sequences (b: beta-sheet). The histidines and the tryptophan involved in the coordination of copper are indicated with arrowheads. The calcium coordinating aspartate residues are indicated with filled circles. The sequence identity and sequence similarity between MopE* and CorA were calculated to 20% and 35%, respectively. The numbers at the right designate the position of the amino acids in the full-length MopE and mature CorA protein. The sequence alignment was generated using ClustalX.

Supplemental fig. S4. Stereo plot illustrating the initial phased and solvent flattened electron density map, including residues 125 – 136 and 203 of the refined MopE* structure. The copper ion is illustrated as a yellow sphere.
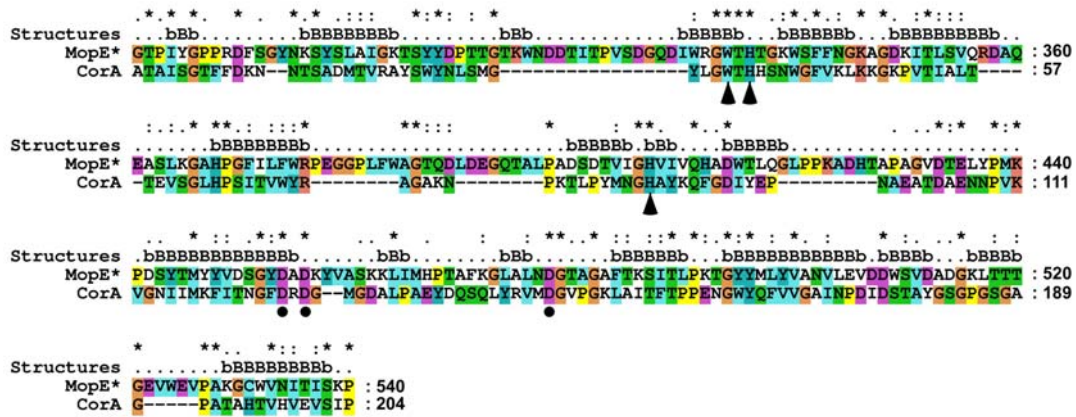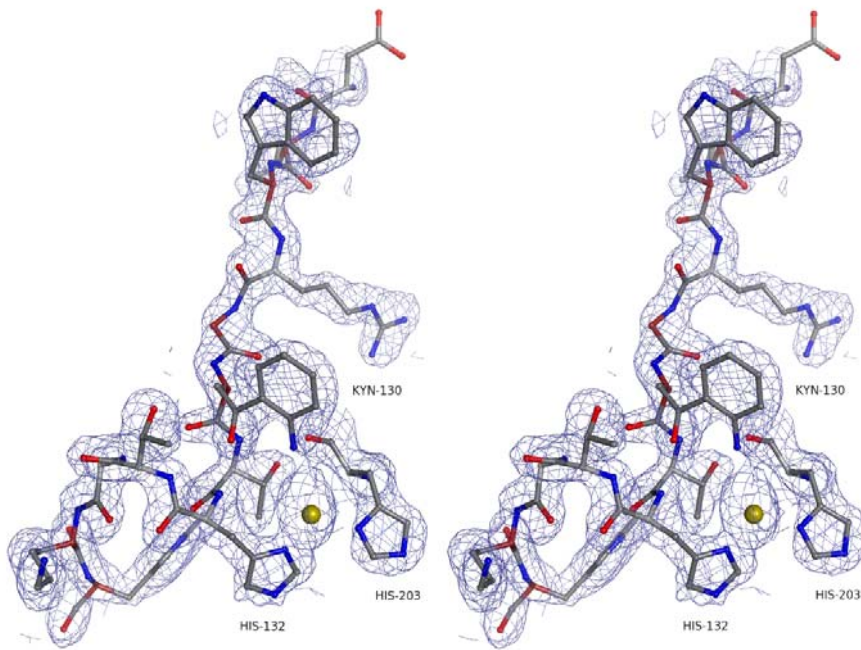
Supplemental figure S1

Supplemental figure S2

A

B

C

D

+4

+2

Kynurenine

Tryptophan

2-amino-4-(2-aminophenyl)-
4-oxobutanoic acid

2-amino-4-(2-aminophenyl)-
pentanoic acid

2-amino-4-(2-aminophenyl)-
pent-4-enoic acid

Supplemental figure S3.

```
            .*.* *.   *.   *.* .:::    *:*:  :  *            : ****  .:*.*.: * *. :*:::
Structures  ...bBb.........bBBBBBBBb.........bBb............bBBBBBb..bBBBBBb.bBBBBBBBBb..
    MopE*    GTPIYGPPRDFSGYNKSYSLAIGKTSYYDPTTGTKWNDDTITPVSDGQDIWRGWTHTGKWSFFNGKAGDKITLSVQRDAQ : 360
    CorA     ATAISGTFFDKN--NTSADMTVRAYSWYNLSMG----------------YLGWTHHSNWGFVKLKKGKPVTIALT---- :  57
                                                                      ▲ ▲

            :.:.* **.: :::*       **:::        *    : **. *..*              . ..*:*  *:*
Structures  .......bBBBBBBBBb.........bBBBBb.bBb....bBBBBb................................
    MopE*    EASLKGAHPGFILFWRPEGGPLFWAGTQDLDEGQTALPADSDTVIGHVIVQHADWTLQGLPPKADHTAPAGVDTELYPMK : 440
    CorA     -TEVSGLHPSITVWYR---------AGAKN--------PKTLPYMNGHAYKQFGDIYEP---------NAEATDAENNPVK : 111
                                                            ▲

            ..  * :: .*:* *     .. *  .    :    : **..* ::* *:.*:* :*. :    * :.   .*   :  :
Structures  .bBBBBBBBBBBBBBBb.......bBb........bBb......bBBBBBb..bBBBBBBBBBBBBBb.bBBBb...bBBBb
    MopE*    PDSYTMYYVDSGYDADKYVASKKLIMHPTAFKGLALNDGTAGAFTKSITLPKTGYYMLYVANVLEVDDWSVDADGKLTTT : 520
    CorA     VGNIIMKFITNGFDRDG--MGDALPAEYDQSQLYRVMDGVPGKLAITFTPPENGWYQFVVGAINPDIDSTAYGSGPGSGA : 189
                        ● ●                          ●

            *      **..  *:: :* *
Structures  ........bBBBBBBBBBb..
    MopE*    GEVWEVPAKGCWVNITISKP : 540
    CorA     G-----PATAHTVHEVSIP  : 204
```

Supplemental figure S4.

An Oxidized Tryptophan Facilitates Copper Binding in *Methylococcus capsulatus* -secreted Protein MopE

Ronny Helland, Anne Fjellbirkeland, Odd Andre Karlsen, Thomas Ve, Johan R. Lillehaug and Harald B. Jensen